



Since January 2020 Elsevier has created a COVID-19 resource centre with free information in English and Mandarin on the novel coronavirus COVID-19. The COVID-19 resource centre is hosted on Elsevier Connect, the company's public news and information website.

Elsevier hereby grants permission to make all its COVID-19-related research that is available on the COVID-19 resource centre - including this research content - immediately available in PubMed Central and other publicly funded repositories, such as the WHO COVID database with rights for unrestricted research re-use and analyses in any form or by any means with acknowledgement of the original source. These permissions are granted for free by Elsevier for as long as the COVID-19 resource centre remains active.



Virtual screening, ADME/Tox predictions and the drug repurposing concept for future use of old drugs against the COVID-19

Lorane Izabel da Silva Hage-Melim^{a,*}, Leonardo Bruno Federico^b,
Nayana Keyla Seabra de Oliveira^a, Viviane Cristina Cardoso Francisco^a, Lenir Cabral Correia^a,
Henrique Barros de Lima^a, Suzane Quintana Gomes^{b,c}, Mariana Pegrucci Barcelos^{b,c},
Isaque Antônio Galindo Francischini^b, Carlos Henrique Tomich de Paula da Silva^{b,c}

^a Laboratory of Pharmaceutical and Medicinal Chemistry (PharMedChem), Federal University of Amapá, Macapá, Amapá, Brazil

^b Computational Laboratory of Pharmaceutical Chemistry, School of Pharmaceutical Sciences of Ribeirão Preto, University of São Paulo, Ribeirão Preto, São Paulo, Brazil

^c Department of Chemistry, School of Philosophy, Sciences and Letters of Ribeirão Preto, University of São Paulo, Ribeirão Preto, São Paulo, Brazil

ARTICLE INFO

Keywords:

SARS-CoV-2
Computational drug repurposing
Coronavirus

ABSTRACT

The new Coronavirus (SARS-CoV-2) is the cause of a serious infection in the respiratory tract called COVID-19. Structures of the main protease of SARS-CoV-2 (M^{pro}), responsible for the replication of the virus, have been solved and quickly made available, thus allowing the design of compounds that could interact with this protease and thus to prevent the progression of the disease by avoiding the viral peptide to be cleaved, so that smaller viral proteins can be released into the host's plasma. These structural data are extremely important for *in silico* design and development of compounds as well, being possible to quick and effectively identify potential inhibitors addressed to such enzyme's structure. Therefore, in order to identify potential inhibitors for M^{pro} , we used virtual screening approaches based with the structure of the enzyme and two compounds libraries, targeted to SARS-CoV-2, containing compounds with predicted activity against M^{pro} . In this way, we selected, through docking studies, the 100 top-ranked compounds, which followed to subsequent studies of pharmacokinetic and toxicity predictions. After all the simulations and predictions here performed, we obtained 10 top-ranked compounds that were again *in silico* analyzed inside the M^{pro} catalytic site, together some drugs that are being currently investigated for treatment of COVID-19. After proposing and analyzing the interaction modes of these compounds, we submitted one molecule then selected as template to a 2D similarity study in a database containing drugs approved by FDA and we have found and indicated Apixaban as a potential drug for future treatment of COVID-19.

1. Introduction

Since the first reports of novel pneumonia (COVID-19) in Wuhan, Hubei province, China, considerable discussion on the origin of the causative virus SARS-CoV-2 (also referred to as HCoV-19) has emerged [1]. Infections with SARS-CoV-2 are now widespread, and efforts to contain the virus are ongoing; however, given the many uncertainties regarding pathogen transmissibility and virulence, the effectiveness of these efforts is unknown. The fraction of undocumented but infectious cases is a critical epidemiological characteristic that modulates the pandemic potential of an emergent respiratory virus [2,3].

SARS-CoV-2 is the seventh coronavirus known to infect humans; SARS-CoV, MERS-CoV and SARS-CoV-2 can cause severe diseases, whereas HKU1, NL63, OC43 and 229E are associated with mild

symptoms [4]. It is improbable that SARS-CoV-2 emerged through laboratory manipulation of a related SARS-CoV-like coronavirus. However, the genetic data irrefutably show that SARS-CoV-2 is not derived from any previously used virus backbone [5]. The general symptoms are similar to SARS and MERS, causing cough, difficulty breathing, fatigue and fever and if not treated properly, eventually death [6,7].

Coronaviruses are enveloped structures, positive single-stranded large RNA viruses that infect humans, but also a wide range of animals. The first virus in the family was described in 1966 by Tyrell and Bynoe, who cultivated the virus obtained of patients with common colds. Due to its morphology with spherical grooves, with a central cap, and superficial projections similar to a solar corona, the name coronavirus (from Latin: corona: crown) was designated. The coronavirus has four subfamilies: alpha-, beta-, gamma- and delta-coronaviruses. While

* Corresponding author.

E-mail addresses: lorane@unifap.br, loranehage@gmail.com (L.I.d.S. Hage-Melim).

<https://doi.org/10.1016/j.lfs.2020.117963>

Received 14 April 2020; Received in revised form 2 June 2020; Accepted 9 June 2020

Available online 11 June 2020

0024-3205/ © 2020 Elsevier Inc. All rights reserved.

alpha- and beta-coronaviruses apparently originate from mammals, in particular from bats, gamma- and delta-viruses originate from pigs and birds. The genome size goes between 26 kb and 32 kb. Among the seven subtypes of coronaviruses that can infect humans, the beta-coronaviruses may cause severe disease and fatalities, whereas alpha-coronaviruses cause asymptomatic or mildly symptomatic infections [7].

During the process of infection, there are two proteases that are essential in the process of maturation and infectivity of the virus. In the case of SARS-CoV-2, sequencing of its genome, revealed the papain-like protease (PL^{Pro}) and the 3-chymotrypsin-like protease (3CL^{Pro}, also known as the main protease-M^{Pro}) [8].

M^{Pro} is one of the most studied therapeutic targets at the present time, as a possible alternative to the fight against coronavirus, proving to be an accessible target for the development of inhibitors [9,10]. M^{Pro} is a cysteine protease composed of three domains (I, II, III), whose main functions are the maturation of viral particles and cleavage of the viral capsid, thus releasing viral polypeptides to the body and contributing to the infection to occur. In its active form, M^{Pro} is a homodimer, containing two protomers, and presents a non-canonical Cys-Hys dyad, located between I and II [11,12].

M^{Pro} is also structurally conserved among the known varieties of coronavirus, with several common characteristics of substrate shared among them, where the amino acids of the substrates C and N termini, are numbered as (-P4-P3-P2-P1 ↓ P1'-P2'-P3'-), and the cleavage site is located between the P1 and P1', with the need for almost all substrates to have a glycine residue located at the position P1 [13,14]. M^{Pro}'s active sites are highly conserved among the different varieties of coronavirus, usually being composed of 4 sites, usually referred to as S1', S1, S2 and S4 [9].

In this work, considering the current pandemic of COVID-19 around the world, we propose use of drug design and lead discovery approaches as well, including virtual screening, ADME/Tox predictions and molecular docking [15], to design new compounds for inhibiting the protease M^{Pro}, involved on the process of viral infection with SARS-CoV-2, thus preventing the viral peptide from being cleaved, and thereby preventing smaller viral charge from being released into the host's plasma [16]. For such purpose, we have compared some repositioned drugs in current clinical studies with SARS-CoV-2 and proposed novel compounds here designed using virtual screening in drug databases.

2. Material and methods

The main steps of the methodological procedure performed in virtual screening are shown in Fig. 1.

2.1. Virtual screening

For virtual screening, we downloaded structure files deposited in the Protein Data Bank (PDB) from the Research Collaboratory for Structural Bioinformatics related to the crystallographic structures of the M^{Pro} (PDB ID: 6LU7, resolution: 2.16 Å), in complex with an inhibitor called N3.

GOLD 2020.1 software (Genetic Optimization for Ligand Docking) performs docking simulations, using a genetic algorithm to generate and select conformers of flexible compounds that bind to the receptor site of a protein or DNA, in addition to be able to use amino acid rotamer libraries in such simulations [17].

First, in order to proceed with the virtual screening experiments, we validated our results by redocking, calculating the root mean-square deviation (RMSD) between the crystallographic pose of the inhibitor and its docking pose. For docking-based virtual screening, we used the following coordinates for the center of the sphere: $x = -10.59$, $y = 13.88$ and $z = 68.56$. Also, a radius of 12.5 Å was here considered.

Two SARS-CoV-2 Targeted Libraries, available by OTAVA Chemicals, has been used, which contain compounds with predicted

activity against M^{Pro}: SARS-CoV-2 Main Protease Targeted Library (SARS-CoV-2-Target, with 1017 compounds) and ML (Machine Learning) SARS Targeted Library (SARS-CoV-2-ML, with 1577 compounds). In sequence, a number of 100 top-ranked hits obtained were reduced, using ADME/Tox filters.

2.2. Prediction of pharmacokinetic properties

For calculation of the pharmacokinetic properties of the drugs under study with SARS-CoV-2 (cobicistat, darunavir, favipiravir, hydroxychloroquine, lopinavir, oseltamivir, remdesivir and ritonavir) as well as of our molecules selected from the two libraries of M^{Pro} inhibitors here used - SARS-CoV-2-Target and SARS-CoV-2-ML, we used the QikProp software [18,19], selecting the following properties, in particular: permeability to the CNS (CNS, logBB and PSA), cell permeability (pCaco-2 and pMDCK), aggregation with serum albumin (logKhsa) and oral absorption (% Human Oral Absorption).

The results obtained with this software were analyzed by comparing the values obtained for the investigated molecules with the average of the values obtained for 95% of the drugs made available in the software databases. Under this comparison, the number of "stars" denotes the number of violations of these ranges of optimal values common to drugs, which are used as references/templates in QikProp [18,19].

In brief, the following properties as well as their ranges of optimal values were considered and here analyzed using the QikProp 4.4 software [19]:

- Stars (similarity to known drugs): 0–2 (high), 3 (medium) e > 4 (low);
- %Human Oral Absorption (%HOA): > 80% (high), 25–80% (medium) e < 25% (low);
- pCaco (intestinal cells): > 500 nm/s (good) e < 25 nm/s (low);
- pMDCK (kidney cells): > 500 nm/s (good) e < 25 nm/s (low);
- logKhsa (binding to human serum albumin): -1,5 (low) a 1,5 (high);
- CNS: -2 (low permeability) e > -2 (high permeability);
- logBB (blood/brain barrier): < -1 (low) e > -1 (easy permeation);
- PSA (Van der Waals surface area): > 60 (does not cross the blood/brain barrier) e < 60 (to cross the blood/brain barrier).

2.3. Prediction of toxicological properties

The DEREK software (Deductive Estimate of Risk from Existing Knowledge) was used to predict the toxicity of the molecules here investigated. This software is an expert-system that uses a methodology capable of making qualitative predictions by searches for 2D similarity shared between the investigated molecule and other structures of the database, which contain reported toxic moieties, predicting, by comparison, the associated toxicity [20]. The results are obtained in the form of alerts that are fired about a possible/potential toxicity of the investigated molecule, which would cause a certain toxic effect on the organism [21].

DEREK's decisions are based on the "knowledge-based expert system" method, for the most diverse and peculiar situations of toxicity, including skin sensitization, hepatotoxicity, nephrotoxicity, carcinogenicity, mutagenicity and other specific toxicities or endpoints [22].

2.4. Molecular docking

Molecular docking simulations between the selected molecules after the previous steps and the biological target M^{Pro} (PDB 6LU7) were performed with the aid of the GOLD 2020.1 software. As previously mentioned, GOLD uses genetic algorithm to generate and select conformers of flexible compounds. For docking, we used the following coordinates for the center of the sphere: $x = -10.59$, $y = 13.88$ and

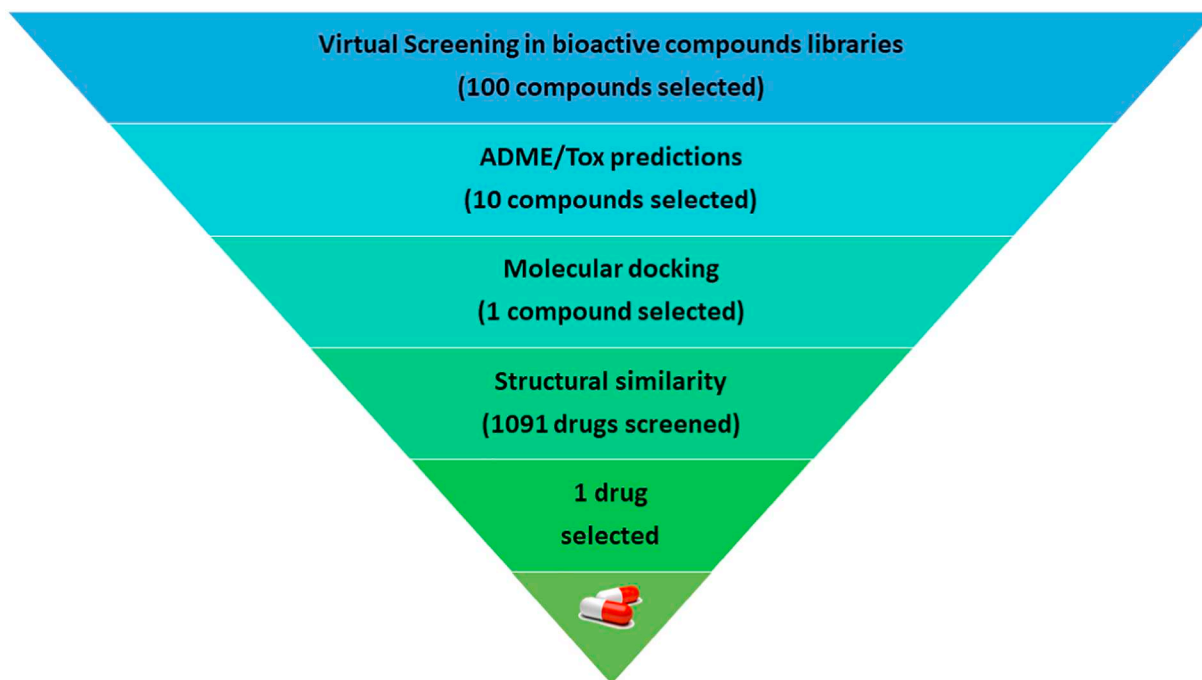


Fig. 1. Workflow with the mains steps of the methodological procedure performed in the virtual screening.

$z = 68.56$, and a radius of 12.5 \AA of docking grid was considered. The co-crystallized ligand, ions and water molecules were removed from the crystal structure before the docking simulations. Prior to the calculations, hydrogens were added to all the compounds, while the respective atomic charges were calculated using the PM3 method, for a better performance/accuracy of the molecular docking.

2.5. Search based on structural similarity

The BindingDB webservice offers the possibility of calculating structural similarity [23] using the Tanimoto coefficient (Tc) [24], based upon JChem fingerprints, resulting in a numerical value of structural similarity between them. As we do not know the active conformation of the molecule here selected as a pivot, 2D similarity provides satisfactory results for the virtual screening step. The Tc analyzed the similarities of the selected molecules, after the results of the previous step, with an FDA library from the webservice itself containing 1091 drugs and classified them according to their similarity. A file of this classification was generated and analyzed using the Discovery Studio software [24] from which a group of molecules with similar activity, above or equal to 40%, was extracted [25].

3. Results and discussion

3.1. Virtual screening in compounds databases

Virtual screening is the computational analogue of the High Throughput Screening (HTS), and it is characterized as the computational screening of chemical compounds deposited in typically large libraries, in order to find molecules that can complement biological targets of resolved structure, selecting the most potent ones, in potential [26]. This technique has very low cost-effective as well as high speed to generate result, giving enormous benefits to pharmaceutical research that needs urgency, such as the SARS-CoV-2 pandemic.

There are different and possible protocols for virtual screening, and a combined use of tools is important so that results could be even more robust, reliable and more likely to be validated/confirmed in *in vitro* assays. Many studies use this technique in the search for chemical

entities for the treatment, for example, of cancer, withdrawal syndrome, neuropathic and inflammatory pain [27–29].

The target structure here used in the screening was M^{pro} (PDB ID: 6LU7), which belongs to a family of enzymes that has been extensively studied from viruses, such as the NS3 protease, from DENGUE virus [30], the protease HIV-1 [31] and others from different viruses that have proteases with known structure as well.

The two libraries here utilized contain compounds with predicted activity against M^{pro}: SARS-CoV-2-Target and SARS-CoV-2-ML. The first library has been designed using structure-based virtual screening (flexible docking), using crystal structure of M^{pro}; the second one has been designed using machine learning (artificial neural networks and Bayesian statistics), based on compounds with known anti-SARS activity.

From each library, 100 hits were selected with highest values of affinity score with M^{pro}, and they are thus selected to the next stages of this work.

3.2. Pharmacokinetic properties analysis

The infection caused by COVID-19 is related to that of SARS, affecting the pneumocytes and macrophages of the lung, which is its target organ. Also, it appears to be related to the ACE2 receptor, which may protect the host against lung injury, as well as to the TMPRSS2 protein, related to facilitating the entry of the virus into the organism, both present in the lung [32]. This information presents us with the peripheral action of the virus, being a requirement for its future therapeutic agent.

Initially, we analyzed the pharmacokinetic predictions of antiviral drugs as well as hydroxychloroquine, currently available (Fig. 2) and also under evaluation of biological activity as well as clinical tests, in the treatment of COVID-19 (Table 1), in order to obtain parameters for comparison among our molecules, selected using virtual screening, whose results are presented in Tables 2 and 3.

All the molecules here investigated showed results with median to high values for oral absorption, as well as median aggregation to plasma proteins. Most of the evaluated drugs showed a prediction of high cellular permeability, both in the results for intestinal cells, as well

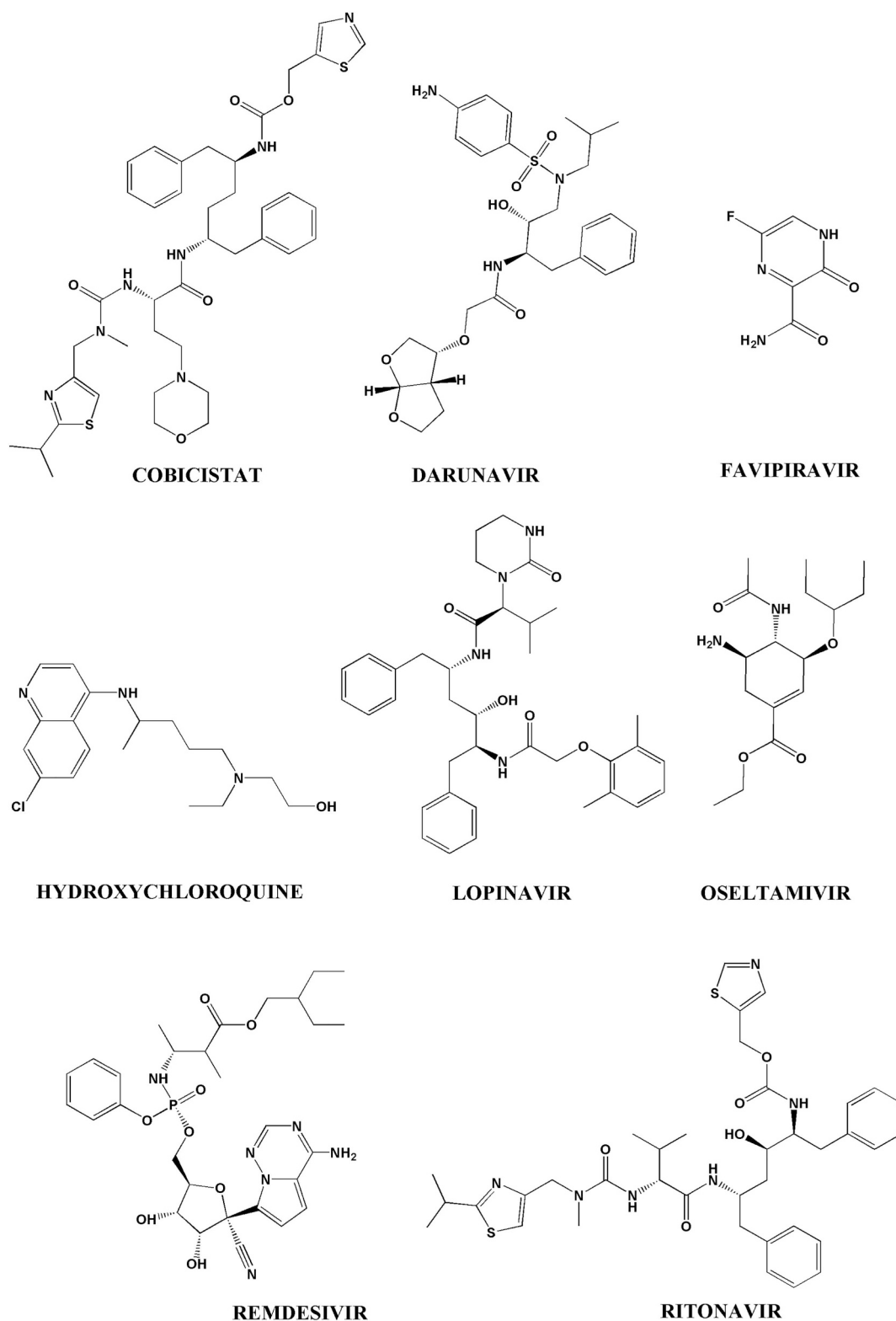


Fig. 2. Chemical structures of the drugs under study in the fight against SARS-CoV-2: cobicistat, darunavir, favipiravir, hydroxychloroquine, lopinavir, oseltamivir, remdesivir and ritonavir.

as for renal cells (pCaco-2 and pMDCK), with the exception only for cobicistat and remdesivir.

Most drugs here evaluated using the QikProp software tend to not permeate the CNS in potential (cobicistat, darunavir, lopinavir, remdesivir and ritonavir), but have high cellular permeability (darunavir, favipiravir, hydroxychloroquine, lopinavir, oseltamivir and ritonavir).

Prediction is median aggregation to protein albumin for all drugs, in addition to prediction of low oral absorption (for cobicistat, darunavir, favipiravir, oseltamivir, remdesivir and ritonavir). Hydroxychloroquine, although a drug indicated for the treatment of rheumatoid arthritis and other inflammatory diseases, has been used with initial satisfactory results in the treatment of COVID-19, and its pharmacokinetic profile, in

Table 1
Pharmacokinetic properties of known drugs.

Molecule	Absorption	Distribution		CNS permeability			
	%HOA	pCaco-2	pMDCK	logKhsa	CNS	logBB	PSA
Cobicistat	49	21	47	0.89	-2	-2.509	162
Darunavir	62	117	81	-0.72	-2	-2.391	128
Favipiravir	61	114	87	-0.75	-1	-0.952	104
Hydroxychloroquine	91	392	488	0.07	1	-0.241	48
Lopinavir	89	887	678	0.61	-2	-1.464	111
Oseltamivir	73	167	116	-0.49	0	-0.544	93
Remdesivir	36	17	6	-0.31	-2	-3.948	193
Ritonavir	69	207	525	0.84	-2	-2.270	151

%HOA = %Human Oral Absorption; pCaco = intestinal cells; pMDCK = kidney cells; logKhsa = binding to human serum albumin; CNS = central nervous system; logBB = blood/brain barrier; PSA = Van der Waals surface area.

comparison to that of antivirals and hydroxychloroquine, despite of indicating permeation to the CNS, has a high cellular distribution, presenting less aggregation to serum albumin (median aggregation), in addition to high oral absorption (similarly to Lopinavir).

Based on the pharmacokinetic profile of antivirals and

hydroxychloroquine as well as knowledge of the virus's peripheral performance, as well as due to their main clinical manifestations, we were able to evaluate the screened molecules.

Regarding the evaluation of the molecules sorted from the SARS-CoV-2-Target library, the 25 molecules with the best pharmacokinetic

Table 2
Prediction of pharmacokinetic properties of molecules selected from the SARS-CoV-2-Target Library.

Molecule	Stars	Absorption	Distribution		CNS permeability			
		%HOA	pCaco-2	pMDCK	logKhsa	CNS	logBB	PSA
SARS-CoV-2-Target_m57	2	93	542	255	1.01	-2	-1.202	96.9
SARS-CoV-2-Target_m66	1	96	606	288	-0.15	-2	-1.205	94.6
SARS-CoV-2-Target_m74	0	95	701	337	-0.40	-2	-1.106	100.7
SARS-CoV-2-Target_m113	0	86	215	234	0.07	-2	-1.253	112.2
SARS-CoV-2-Target_m135	0	91	308	138	0.59	-2	-1.017	118.4
SARS-CoV-2-Target_m152	1	77	117	80	-0.31	-2	-1.792	126.4
SARS-CoV-2-Target_m157	0	88	231	251	0.15	-2	-1.469	112.7
SARS-CoV-2-Target_m172	0	96	486	227	0.48	-2	-1.190	113.6
SARS-CoV-2-Target_m351	0	93	353	282	0.35	-2	-1.156	92.8
SARS-CoV-2-Target_m379	0	95	368	272	0.44	-2	-1.128	84.8
SARS-CoV-2-Target_m454	0	78	104	120	0.07	-2	-1.519	115.6
SARS-CoV-2-Target_m555	0	100	603	286	0.66	-2	-1.045	84.8
SARS-CoV-2-Target_m582	1	100	462	302	0.71	-2	-1.272	111.2
SARS-CoV-2-Target_m603	2	87	92	37	0.68	-2	-2.084	139.5
SARS-CoV-2-Target_m648	0	91	356	162	0.19	-2	-1.405	110.3
SARS-CoV-2-Target_m703	2	88	312	140	1.02	-2	-1.563	125.2
SARS-CoV-2-Target_m743	0	91	198	193	0.81	-2	-1.125	89.9
SARS-CoV-2-Target_m752	0	100	674	323	0.79	-2	-1.009	91.5
SARS-CoV-2-Target_m808	2	90	166	71	0.69	-2	-1.715	117.7
SARS-CoV-2-Target_m824	0	94	398	183	0.47	-2	-1.196	99.2
SARS-CoV-2-Target_m825	1	100	568	268	0.65	-2	-1.099	102.6
SARS-CoV-2-Target_m830	1	65	58	56	0.49	-2	-2.041	138.5
SARS-CoV-2-Target_m882	1	100	306	191	0.85	-2	-1.559	122.9
SARS-CoV-2-Target_m888	2	100	576	675	0.74	-2	-1.034	105.8
SARS-CoV-2-Target_m896	1	100	464	379	0.83	-2	-1.233	115.9

%HOA = %Human Oral Absorption; pCaco = intestinal cells; pMDCK = kidney cells; logKhsa = binding to human serum albumin; CNS = central nervous system; logBB = blood/brain barrier; PSA = Van der Waals surface area; Light green = average; Light red = medium.

Table 3
Prediction of pharmacokinetic properties of molecules selected from the SARS-CoV-2-ML Library.

Molecule	Stars	Absorption		Distribution		CNS permeability		
		%HOA	pCaco-2	pMDCK	logKhsa	CNS	logBB	PSA
SARS-CoV-2-ML_m13	0	95	401	184	0.38	-2	-1.172	103.73
SARS-CoV-2-ML_m188	0	100	505	359	0.62	-2	-1.022	102.23
SARS-CoV-2-ML_m239	0	87	237	292	-0.06	-2	-1.448	103.47
SARS-CoV-2-ML_m250	1	100	672	322	0.53	-2	-1.120	106.39
SARS-CoV-2-ML_m388	0	92	269	193	0.46	-2	-1.311	84.16
SARS-CoV-2-ML_m485	0	92	155	195	0.62	-2	-1.544	113.91
SARS-CoV-2-ML_m492	0	85	228	421	-0.07	-2	-1.186	114.44
SARS-CoV-2-ML_m494	0	93	534	251	0.13	-2	-1.126	89.43
SARS-CoV-2-ML_m498	0	82	156	303	-0.05	-2	-1.385	115.46
SARS-CoV-2-ML_m500	1	94	324	282	0.35	-2	-1.127	87.46
SARS-CoV-2-ML_m1169	0	89	315	143	-0.14	-2	-1.527	111.04
SARS-CoV-2-ML_m1173	0	86	302	234	0.10	-2	-1.111	92.43
SARS-CoV-2-ML_m1269	2	100	459	213	0.45	-2	-1.419	102.56
SARS-CoV-2-ML_m1350	0	80	143	113	0.13	-2	-1.257	112.95
SARS-CoV-2-ML_m1444	0	86	303	136	0.07	-2	-1.192	95.86
SARS-CoV-2-ML_m1453	0	100	771	651	0.31	-2	-1.029	91.30
SARS-CoV-2-ML_m1575	0	91	399	184	0.34	-2	-1.113	91.54

%HOA = %Human Oral Absorption; pCaco = intestinal cells; pMDCK = kidney cells; logKhsa = binding to human serum albumin; CNS = central nervous system; logBB = blood/brain barrier; PSA = Van der Waals surface area.

profiles predicted are shown in Table 2. Considering the number of “stars”, all the results here obtained indicate high reliability, indicating chemical similarity to known drug molecules of the QikProp software database.

Such as for the permeability to CNS, we chose to work with those molecules for which there is a prediction to act at the peripheral level, selecting the molecules that presented results for the three parameters evaluated (CNS, QPlogBB and PSA), with a prediction of not crossing the blood-brain barrier, since peripheral action is sought due to the clinical characteristics of the disease.

It can be seen that, compared to the profile of antivirals and hydroxychloroquine, the profile obtained for molecules from the SARS-CoV-2-Target library is even more satisfactory and adequate, in potential. Cell distribution was predicted from median to high for Caco-2 as well as MDCK cells, median binding to plasma proteins and median to high %HOA.

Evaluating the set of predictions made here, the 17 molecules, selected from the SARS-CoV-2-ML library and containing the best pharmacokinetic profiles are shown in Table 3. Considering the number of “stars”, all molecules obtained highly reliable results.

All molecules selected from the SARS-CoV-2-ML library that not showed permeability to CNS, in potential, showed indicative results for high oral absorption, whereas for none of them high aggregation to plasma proteins was predicted.

Such as for permeability to CNS, those with prediction to act at the peripheral level were selected following the three parameters evaluated (CNS, logBB and PSA), for which the prediction was median to high cell distribution, both for intestinal cells as well as pCaco-2 and pMDCK cells.

In comparison to the predicted profile for antivirals and hydroxychloroquine, it can be noted that the profile of cell distribution (pCaco-2 and pMDCK), logKhsa and %HOA of SARS-CoV-2-ML molecules is also superior.

Young et al. [33] reported in their study the result of the combined use of the antivirals lopinavir and ritonavir as pharmacological alternatives initially used to treat atypical pneumonia caused by COVID-19. Unfortunately, among the group of patients evaluated, there was no proven efficacy in the treatment, with patients who had a clinical evolution to acute respiratory failure, in addition to no reduction in

viral charge, which remained similar to that of untreated patients. Such information indicates the urgent need for a specific and effective pharmacological alternative against this pandemic disease.

3.3. Toxicological properties analysis

Computational tools used to predict the toxic potential of the most varied molecules can have a significant impact on the discovery and development of drugs, and toxicity is one of the fundamental parameters for the continuation of research in drug design and development [34].

Zhang et al. [35] revealed a high-resolution structure of α -ketoamide bound to the protease, responsible for a block of the viral RNA replication. They report that α -ketoamide has a prolonged half-life in the blood plasma. In addition, they tested their main inhibitory compound in mice, finding that inhalation was well tolerated and that the mice had no adverse effects. They suggested, therefore, that since human proteases with a similar cleavage specificity are not known, it is unlikely that this class of inhibitors will be toxic, which results in a useful structure for the development of drugs to combat the new coronavirus.

In this study, DEREK software was used to predict the toxicological properties of the drugs under study with SARS-CoV-2 (cobicistat, darunavir, favipiravir, hydroxychloroquine, lopinavir, oseltamivir, remdesivir and ritonavir) as well as the molecules selected from libraries of M^{Pr}o inhibitors. This software has a system that makes predictions from a qualitative point of view and, thus, alerts are fired about the possible toxic action of the analyzed chemical compounds, being able to interpret toxicophoric substructures present in the compounds as possible inducers of certain types of toxicity, such as mutagenicity, carcinogenicity, skin sensitization, irritation, reproductive effects, neurotoxicity, among others, through correlation rules established by the software.

For the drugs here investigated, the fired alerts are described below:

- Cobicistat: plausible hepatotoxicity, probably due to the thiazole or derivative and carbamate group, in addition to inhibition of the HERG channels.
- Darunavir: plausible hepatotoxicity, probably due to the presence of

the 4-Aminophenylsulphonamide or 4-aminophenylsulphone group, carcinogenicity, mutagenicity, chromosomal damage, genotoxicity and thyroid toxicity.

- Favipiravir: no toxicity alerts were fired.
- Hydroxychloroquine: plausible hepatotoxicity, probably due to the quinoline group, inhibition of HERG channels, carcinogenicity and irritation of the respiratory tract (ethanolamine), in addition to ocular toxicity (4-Aminoquinoline derivative).
- Lopinavir: glucocorticoid receptor agonist, in addition to teratogenicity.
- Oseltamivir: chromosomal damage (alpha, beta-unsaturated ester)
- Remdesivir: plausible hepatotoxicity (Organophosphorus di tri-ester), cholinesterase inhibition and irritation of the gastrointestinal tract.
- Ritonavir: plausible hepatotoxicity (Thiazole and carbamate), glucocorticoid receptor agonist and teratogenicity.

Favipiravir is an antiviral agent that selective and potently inhibits RNA-dependent RNA polymerase (RdRp) from RNA viruses. Favipiravir was discovered by HTS screening of the chemical library for antiviral activity against the influenza virus by Toyama Chemical Co., Ltd. Favipiravir undergoes intracellular phosphoribosylation to be an active form, favipiravir-RTP (favipiravir- RTP (favipiravir ribofuranosyl-5B-triphosphate), which is recognized as a substrate for RdRp that inhibits the activity of RNA polymerase. Because the catalytic domain of RdRp is conserved among various types of RNA viruses, this mechanism of action supports a broader spectrum broad range of antiviral activities of favipiravir. Favipiravir is effective against a wide variety of influenza virus types and subtypes, including strains resistant to existing anti-influenza drugs, and is potentially promising for specifically intractable RNA viral infections [36].

On the other hand, favipiravir presents a risk of teratogenicity and embryotoxicity. Therefore, the Ministry of Health, Labor and Welfare has granted conditional marketing approval with strict regulations for its production and clinical use [37].

In a study by Furuta et al. [38], it was found that favipiravir has a potent and selective inhibitory activity against the influenza virus. In an *in vitro* plaque reduction assay, favipiravir showed potent inhibitory activity against influenza A, B and C viruses, with 50% inhibitory concentrations (IC₅₀) of 0.013 to 0.48 g/ml, while showing no cytotoxicity in concentrations up to 1000 g/ml in MDCK cells.

Hydroxychloroquine and chloroquine are respectively used in the treatment of malaria and rheumatoid arthritis, systemic lupus erythematosus and inflammatory rheumatic diseases, and are considered weak bases. These drugs interfere with lysosomal activity and autophagy, interact with membrane stability, and alter signaling pathways and transcriptional activity, which can result in the inhibition of cytokine production and the modulation of certain costimulatory molecules. These modes of action, together with the chemical properties of the drug, can explain the clinical efficacy and known adverse effects (such as retinopathy and cardiac arrhythmia) of these drugs [39].

Cortegiani et al. [40] systematically reviewed the evidence on chloroquine and hydroxychloroquine for the treatment of COVID-19. They found that chloroquine appears to be effective in limiting SARS-CoV-2 replication *in vitro*. However, in this present study, hydroxychloroquine presented plausible hepatotoxicity probably due to the quinoline group, inhibition of the HERG channels, carcinogenicity and irritation of the respiratory tract (ethanolamine) and ocular toxicity (derived from 4-Aminoquinoline), demonstrating the high degree of toxicity of this drug.

Reaffirming, Yam and Kwok [41] cite that one of the main side effects of hydroxychloroquine is ocular toxicity, which can adversely affect the cornea, the ciliary body and the retina. On the other hand, recent studies suggest that the internal retina is not significantly damaged with the development of human hydroxychloroquine toxicity [42].

Toxicity of ethanolamine was studied by the Toxicology Committee in 1967. The study by Weeks et al. [43] indicated that skin and eye irritation in addition to immediate signs of irritability and restlessness followed by CNS depression were the main adverse effects observed in experimental animals not anesthetized and exposed to ethanolamine at 12–26 ppm for 24 h. Continuous exposure to 5–6 ppm produced some behavioral changes in the animals, but only after 2–3 weeks of exposure.

Sang et al. [44] chose six approved anti-HIV-1 drugs to investigate their interactions with M^{PRO} as well as to assess the potential to become clinical drugs for the new coronavirus pneumonia (COVID-19) caused by SARS-CoV-2 infection. They found that darunavir has the best binding affinity for M^{PRO} among all tested inhibitors, indicating that it has the potential to become a clinical drug to treat COVID-19. However, the results of the toxicological properties of this drug point out warnings such as hepatotoxicity and mutagenicity as well, which deserve attention.

Qamar et al. [16] examined a database of medicinal plants containing 32,297 phytochemicals as potential antivirals and selected nine promising drug-free and non-toxic natural products that can inhibit M^{PRO} activity and, therefore, virus replication. The nine products are: 5,7,3',4'-Tetrahydroxy-2'-(3,3-dimethylallyl) isoflavone; Myricitrin; Methyl rosmarinat; 3,5,7,3',4',5'-hexahydroxyflavanone-3- β -D-glucopyranoside; (2S)-Eriodictyol 7-O-(6'-O-galloyl)- β -D-glucopyranoside; Calcearioside B; Micricetin 3-O- β -D-glucopyranoside; Licoleafol and Amaranth.

A study by Singh and Konwar [45] performed molecular coupling of the epigallocatechin gallate (EGCG) and its analogs against the virus M^{PRO} enzyme. Previous reports have indicated EGCG as an M^{PRO} inhibitor, but with a low oral bioavailability, thus stimulating its molecular optimization. According to these reported data, the analogues bound to the enzyme active site and these improved the pharmacological properties, estimated in comparison with the EGCG. In predicting ADME/Tox of the analogs, the study revealed that they have improved pharmacological properties.

Fisher et al. [46] computationally examined a library of > 687 million compounds for binding to the crystal structure of M^{PRO}. They evaluated the potential toxic effects of the compounds due to the interaction with 16 known drugs, and then made a final selection of 11 compounds. Compounds with an improvement in binding free energy in contrast to the cocrystallized inhibitor were considered for their potential toxicity. Among the compounds evaluated, the authors found that the natural compound containing the lowest value of free binding energy was taxifoline.

According to Jo et al. [47], coronaviruses have been the target of some flavonoids, where it is assumed that the antiviral activity of some flavonoids against CoVs is directly caused by the inhibition of M^{PRO}.

Regarding the screened molecules, of 100 molecules selected from the SARS-CoV-2-Target library, 33 did not present any human toxicity alert (Table 4), 17 presented one alert, 17 presented two alerts and 15 molecules presented three alerts. On the other hand, from the SARS-CoV-2-ML library, 21 molecules showed no warning signs (Table 4), 24 showed only one alert, 20 showed two warning signs, and 16 molecules presented with three alerts.

3.4. Molecular docking

Considering the analysis of pharmacokinetic and toxicological properties, we selected 10 molecules (Fig. 3), 9 from the SARS-CoV-2-Target library (m57, m74, m113, m135, m152, m351, m603, m808 and m824) and 1 from the SARS-CoV-2-ML library (m494) (Supplementary material, Table 5), in order to analyze intermolecular interactions that could occur with M^{PRO}, in comparison with favipiravir, which presents satisfactory results, as well as hydroxychloroquine, since it is a drug that presents results in literature as a potential drug for treatment of COVID-19 [48].

Evaluating the amino acids HIS41 and CYS145, present in the active

Table 4
Molecules selected from SARS-CoV-2 libraries that did not present toxicity alerts according to the DEREK software.

SARS-CoV-2-Target	SARS-CoV-2-ML
m57	m246
m71	m252
m74	m258
m106	m344
m113	m479
m120	m480
m135	m484
m152	m487
m168	m490
m250	m494
m262	m529
m320	m726
m351	m950
m378	m1201
m385	m1312
m413	m1324
m418	m1345
m431	m1418
m438	m1447
m541	m1456
m553	m1467
m579	
m601	
m603	
m711	
m761	
m808	
m824	
m830	
m838	
m868	
m972	
m980	

site of said protease (Protomer A) [49], they were used with the purpose of comparing the docking results, in addition to the amino acid residues that showed the highest number of interactions with ligands. All the molecules interact with the amino acid residue CYS145, with the exception of m74. However, with the amino acid residue HIS41, only the hydroxychloroquine drug and the screened molecules m57, m113, m135 and m808 showed interactions.

Molecular docking results indicated the lowest number of interactions for the drug favipiravir - 6 interactions, being 1 hydrophobic and 5 hydrogen bonds with the amino acids GLY143, SER144, CYS145 and HIS163; and 5 interactions for m824, 2 of which are hydrophobic and 3 are hydrogen bonds with the amino acids GLY143, SER144, CYS145 and MET165. The observed score value was 38.3 for the drug favipiravir, which is the lowest one observed among the molecules here investigated, and 70.18 for m824.

Hydroxychloroquine and m494 molecules showed the highest number of interactions, 14 for each. For the first, 11 hydrophobic interactions and 3 hydrogen bonds were observed with amino acid residues HIS41, MET49, GLY143, CYS145, HIS163, MET165 and GLU166, with a score value of 66.07. Each of the amino acid residues HIS41, MET49, CYS145 and MET165 had at least two points of hydrophobic interaction with hydroxychloroquine, and GLU166 had two points of hydrogen bonding. GLY143 presented only one hydrogen bonding point and HIS163 had a hydrophobic interaction point with the inhibitor.

For m494, 4 hydrophobic interactions and 10 hydrogen bonds were identified with the amino acid residues LEU141, SER144, CYS145, MET165, GLU166, ARG188, GLN189 and THR190, obtaining a score value of 74.42. In this case, the amino acid residues MET165 and GLN189 had two points of hydrophobic interaction with SARS-CoV-2-ML_m494, while SER144 and CYS145 had two points of hydrogen bonding. The GLN189 residue, in addition to the two hydrophobic

interactions, also showed a hydrogen bond with the inhibitor. Finally, the amino acid residues LEU141, GLU166, ARG188 and THR190 presented a hydrogen bonding point with the inhibitor, each one.

Molecules with intermediate number of interactions were m74 (8), m135 (8), m351 (9), m603 (8) and m808 (8) with satisfactory score values for the best pose equal to 75.3; 61.41; 70.36; 68.45 and 73.55, respectively. M74 did not interact with the amino acid residues belonging to the catalytic site, unlike the m135 and m808 molecules that managed to interact with the HIS41 and CYS145 residues.

The molecule that had the highest score value, 80.75, was m152. A total of 7 interactions were observed, with 4 hydrophobic interactions and 3 hydrogen bonds. In this case, each of the amino acid residues MET49, CYS145, GLU166 and LEU167 presented only one point of interaction as an inhibitor, these interactions being hydrophobic for MET49 and CYS145, and hydrogen bond for GLU166 and LEU167. The amino acid residue PRO168 was the only one that showed multiple interactions with the m152 inhibitor, two hydrophobic interactions and one hydrogen bond. However, there was no interaction with the amino acid residue HIS41 belonging to the catalytic site of M^{pro} .

The m57 and m113 molecules stand out for having a satisfactory number of interactions and score value, emphasizing that the first was the molecule studied that showed interaction with the largest number of amino acid residues (8). For m57, 12 interactions were observed, 6 of them hydrophobic and 6 of hydrogen bonds the amino acids LEU27, HIS41, GLY143, CYS145, MET165, GLU166, PRO168 and GLN189, and the score value obtained for the best pose was 73, 69. For m113, 10 interactions were identified, 9 of them hydrophobic and 1 hydrogen bond with the amino acids HIS41, MET49, CYS145, MET165, GLU166, PRO168 and GLN189, and a score value of 72.57. It is important to note that both had score values higher than those obtained for the drugs studied.

Considering the amino acids GLY143, CYS145, HIS163, HIS164, GLU166, GLN189, and TYR190 that bind with the crystallographic inhibitor N3, only the m494 molecule interacted with the TYR190 residue. For the amino acid GLY143, there was interaction only with the favipiravir, hydroxychloroquine, m57 and m824 molecules. For the amino acid CYS145, all molecules interacted, with the exception of m74. The HIS163 residue interacted only with the favipiravir, hydroxychloroquine, m74 and m135 molecules. No linker interacted with the amino acid residue HIS164. The amino acid residue GLU166 showed interaction with all molecules, except with favipiravir and m824. The GLN189 residue, on the other hand, interacted only with the m57, m113 and m494 molecules.

The amino acid residues CYS145, MET165, PRO168 and GLN189 proved to be capable of making multiple chemical interactions of different nature with the inhibitors. Its multiple interactions are present both in the cases in which the inhibitors had the highest number of interactions with the target, and in the case in which the inhibitor presented the highest score value among the twelve selected molecules.

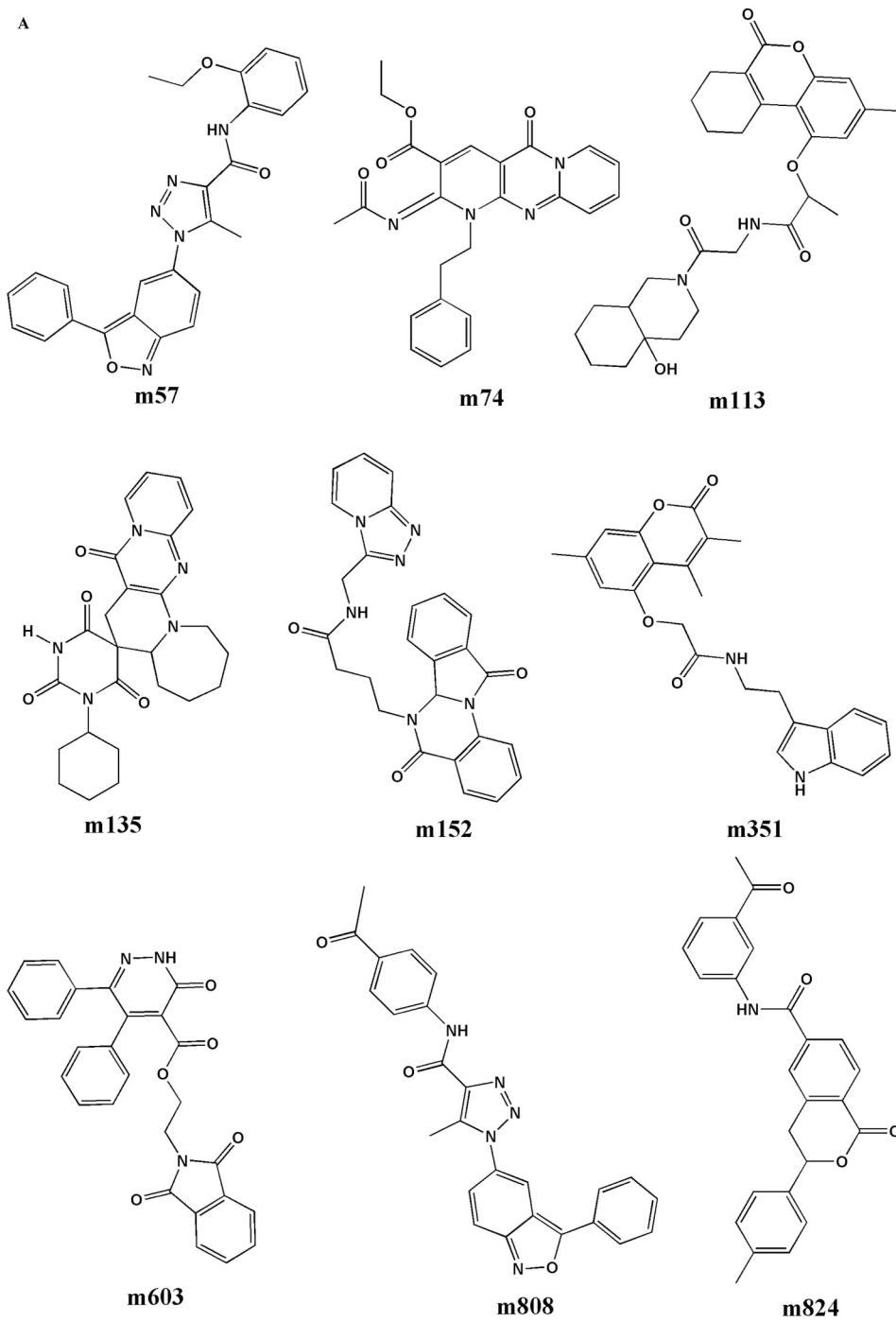
Therefore, the amino acid residues MET165, PRO168 and GLN189 showed their relevance in multiple interactions of different chemical natures between the inhibitor and the target, in addition to the HIS41 and CYS145 residues already belonging to the active site of M^{pro} , and we can select the m57 molecule as the most promising drug candidate for treatment of COVID-19 (Fig. 4).

3.5. Search based on structural similarity

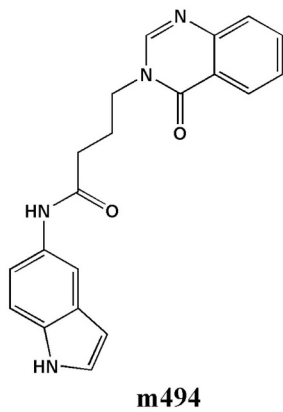
Similar Property Principle (SPP) states that molecules that are similar in overall structure are likely to have similar biological activity [50].

With the similarity analysis, it was possible to select the drug Apixaban, which showed 42% similarity with the selected molecule m57. Then, molecular docking calculations were performed for the target M^{pro} (Fig. 5), obtaining 12 interactions, 3 with the catalytic dyad, HIS41 and CYS145, and 9 other interactions with 8 more amino acids

A



B



(caption on next page)

Fig. 3. Molecules selected from libraries: A) SARS-CoV-2-Target - m57, m74, m113, m135, m152, m351, m603, m808 and m824, B) 1 from the SARS-CoV-2-ML library - m494.

(MET49, LEU141, ASN142, GLY143, HIS163, MET165, PRO168 and ARG188), with a score value of 75.26.

Apixaban is an anticoagulant, acts by selectively inhibiting the activated factor Xa in a reversible manner and has an oral bioavailability of ~50%. It is administered as twice daily dose. It is excreted in urine and feces. Apixaban is useful in atrial fibrillation, venous thromboembolism, and pulmonary embolism. Bleeding is the major side effect of Apixaban [51].

In a clinical study made by Tang et al. [52] with 449 patients with severe COVID-19, 99 of them received heparin (mainly with low molecular weight heparin, LMWH) for 7 days or longer. The 28-day mortality of heparin users were lower than nonusers in patients with SIC score ≥ 4 or D-dimer > 6 fold of upper limit of normal. They concluded that anticoagulant therapy, mainly with LMWH, appears to be associated with better prognosis in severe COVID-19 patients meeting sepsis-induced coagulopathy (SIC) criteria or with markedly elevated D-dimer.

Injectable anticoagulants such as heparin are prescribed when anticoagulation therapy is required for short duration. Absence of oral

form of heparin makes it impractical for long-term use. As an alternative, warfarin and coumarone derivatives are the best available oral anticoagulants in market [51]. It has been found that Apixaban has superiority over warfarin and aspirin in terms of efficacy and safety [53].

In the present study, a toxicity prediction study using DEREK software was done and no alerts were fired for the drug Apixaban.

4. Conclusion

In this work, we present proposals for new potential M^{pro} inhibitors of the SARS-CoV-2 virus (PDB ID: 6LU7) as an alternative treatment for COVID-19. These compounds were designed from virtual screening experiments in two compound databases, one being previously built from docking compounds with M^{pro} , and the other was built from compounds with known anti-SARS activity. From these virtual screening experiments here performed, we selected the 100 top-ranked hits from each database. Their ADME/Tox properties were calculated and compared to those of drugs currently being tested with COVID-19,

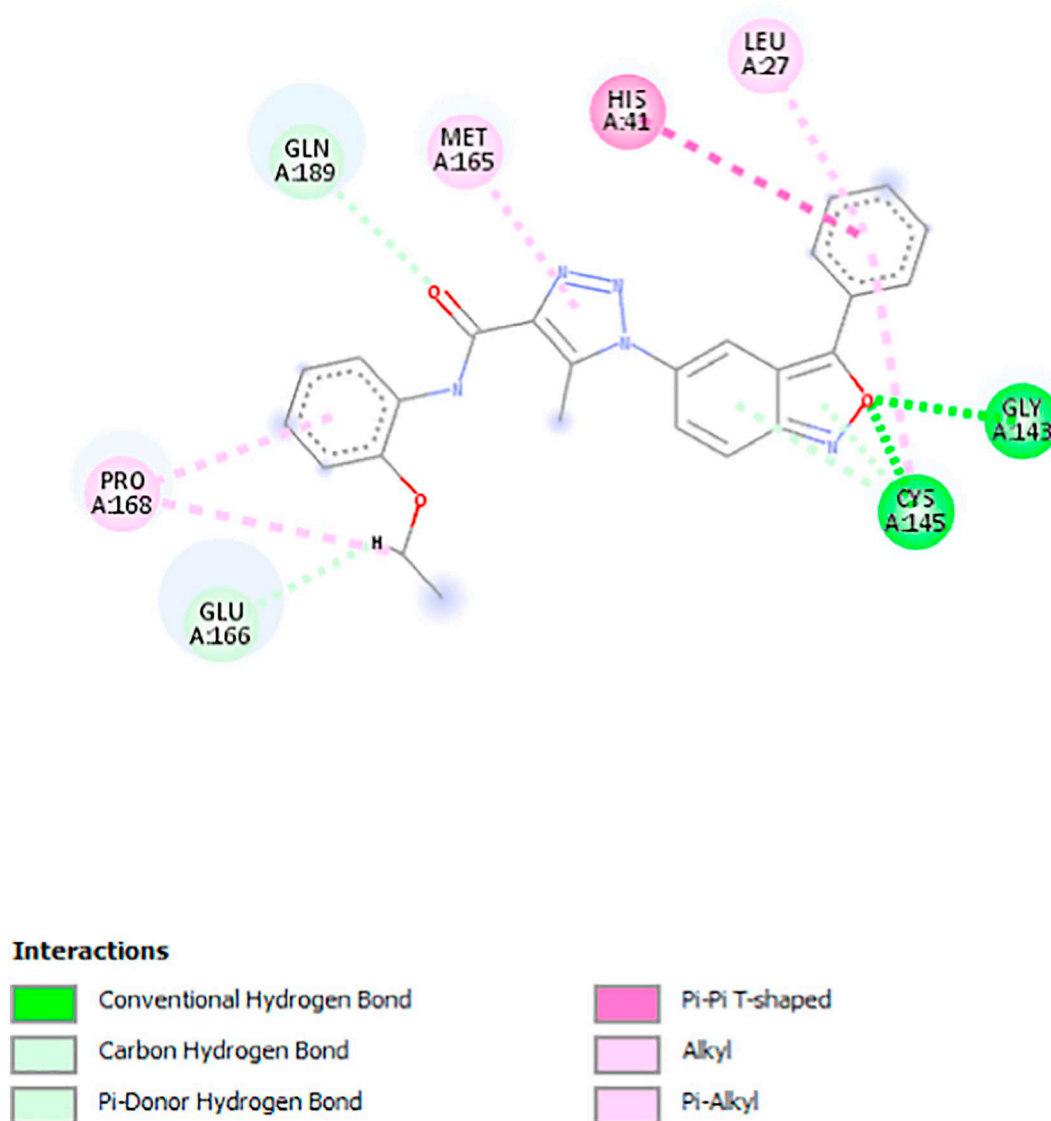


Fig. 4. Intermolecular interactions between the drug candidate molecule (m57) for treatment of COVID-19 and the amino acid residues of the therapeutic target M^{pro} .

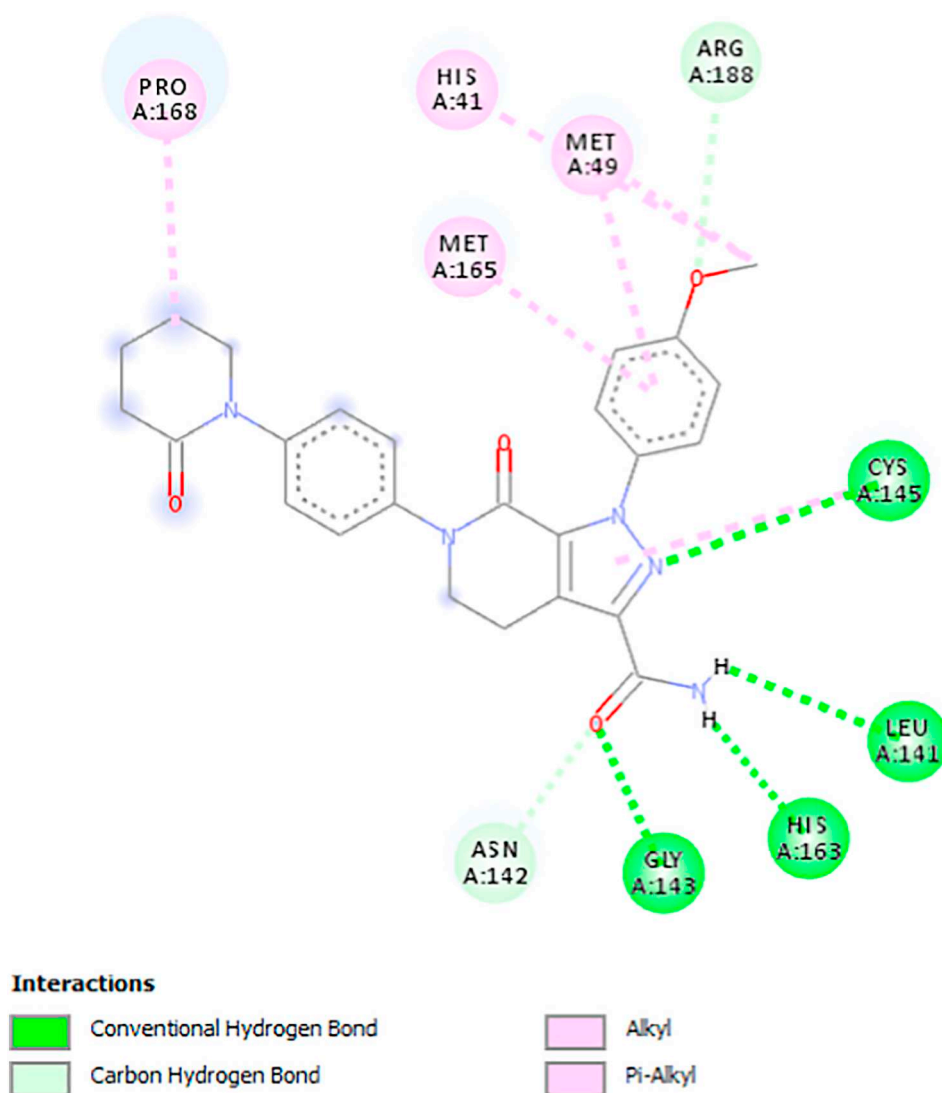


Fig. 5. Intermolecular interactions between the drug Apixaban and the amino acid residues of the therapeutic target M^{pro} .

by attempting to reposition of the function, among known antivirals and hydroxychloroquine, a drug used in the treatment of rheumatoid arthritis as well as other inflammatory diseases. Our compounds designed and here presented showed pharmacokinetic and toxicological properties even more satisfactory and suitable than the drugs currently in test with COVID-19, in addition to maintain a network of favorable intermolecular interactions with the M^{pro} of the new coronavirus, according to the docking studies here performed with such enzyme. Also, an inhibitor was selected serving as a template for study of similarity and drug repurposing and it was possible to identify Apixaban, an known anticoagulant administered by the oral route, which shows very promising results for future treatment of COVID-19. Due to the suitable pharmacotherapeutic profile as well as very low toxicity and adverse effects, thus estimated for our potential M^{pro} inhibitors of the SARS-CoV-2 virus, we suggest our most promising compound as well as Apixaban as proposals for alternative tests with COVID-19, for future treatment of patients affected with this severe acute respiratory syndrome.

Supplementary data to this article can be found online at <https://doi.org/10.1016/j.lfs.2020.117963>.

Declaration of competing interest

There is no conflict of interest.

Acknowledgements

We acknowledge support from Conselho Nacional de Desenvolvimento Científico e Tecnológico (CNPq), Coordenação de Aperfeiçoamento de Pessoal de Nível Superior (Capes) and Drug Technologies.

References

- [1] S. Jiang, Z. Shi, Y. Shu, J. Song, G.F. Gao, W. Tan, D. Guo, A distinct name is needed for the new coronavirus, *Lancet* 395 (2020) 949, [https://doi.org/10.1016/S0140-6736\(20\)30419-0](https://doi.org/10.1016/S0140-6736(20)30419-0).
- [2] J.F.W. Chan, S. Yuan, K.H. Kok, K.K.W. To, H. Chu, J. Yang, ... K.Y. Yuen, A familial cluster of pneumonia associated with the 2019 novel coronavirus indicating person-to-person transmission: a study of a family cluster, *The Lancet* 395 (2020) 514–523, [https://doi.org/10.1016/S0140-6736\(20\)30154-9](https://doi.org/10.1016/S0140-6736(20)30154-9).
- [3] R. Li, S. Pei, B. Chen, Y. Song, T. Zhang, W. Yang, J. Shaman, Substantial undocumented infection facilitates the rapid dissemination of novel coronavirus (SARS-CoV2), *Science* (2020), <https://doi.org/10.1126/science.abb3221>.
- [4] V.M. Corman, D. Muth, D. Niemeyer, C. Drosten, Hosts and sources of endemic human coronaviruses, *Adv. Virus Res.* 100 (2018) 163–188, <https://doi.org/10.1016/bs.aivir.2018.01.001>.
- [5] F. Almazán, I. Sola, S. Zuñiga, S. Marquez-Jurado, L. Morales, M. Becares,

- L. Enjuanes, Coronavirus reverse genetic systems: infectious clones and replicons, *Virus Res.* 189 (2014) 262–270, <https://doi.org/10.1016/j.virusres.2014.05.026>.
- [6] S. Belouzard, J.K. Millet, B.N. Licitra, G.R. Whittaker, Mechanisms of coronavirus cell entry mediated by the viral spike protein, *Viruses* 4 (2012) 1011–1033, <https://doi.org/10.3390/v4061011>.
- [7] T.P. Velavan, C.G. Meyer, The COVID-19 epidemic, *Tropical Med. Int. Health* 25 (2020) 278–280, <https://doi.org/10.1111/tmi.13383>.
- [8] R. Arya, A. Das, V. Prashar, M. Kumar, Potential inhibitors against papain-like protease of novel coronavirus (SARS-CoV-2) from FDA approved drugs, *ChemRxiv* (2020), <https://doi.org/10.26434/chemrxiv.11860011.v2>.
- [9] W. Dai, B. Zhang, H. Su, J. Li, Y. Zhao, X. Xie, Z. Jin, J. Peng, F. Liu, C. Li, Y. Li, F. Bai, H. Wang, X. Cheng, X. Cen, S. Hun, X. Yang, J. Wang, X. Liu, G. Xiao, H. Jiang, Z. Rao, L.K. Zhan, Y. Xu, H. Yang, H. Liu, Structure-based design of antiviral drug candidates targeting the SARS-CoV-2 main protease, *Science* 4489 (2020) 1–10, <https://doi.org/10.1126/science.abb4489>.
- [10] J.C. Crosby, M.A. Heimann, S.L. Burleson, B.C. Anzalone, J.F. Swanson, D.W. Wallace, C.J. Greene, COVID-19: a review of therapeutics under investigation, *Journal of the American College of Emergency Physicians Open* (2020), <https://doi.org/10.1002/emp2.12081>.
- [11] K. Anand, G.J. Palm, J.R. Mesters, S.G. Siddell, J. Ziebuhr, R. Hilgenfeld, Structure of coronavirus main proteinase reveals combination of a chymotrypsin fold with an extra α -helical domain, *EMBO J.* 21 (2002) 3213–3224, <https://doi.org/10.1093/emboj/cdf327>.
- [12] K. Anand, J. Ziebuhr, P. Wadhvani, J.R. Mesters, R. Hilgenfeld, Coronavirus main proteinase (3CLpro) structure: basis for design of anti-SARS drugs, *Science* 300 (2003) 1763–1767, <https://doi.org/10.1126/science.1085658>.
- [13] F.G. Hayden, R.B. Turner, J.M. Gwaltney, K. Chi-Burris, M. Gersten, P. Hsueh, G.J. Smith III, L.S. Zelman, Phase II, randomized, double-blind, placebo-controlled studies of rupintrivir nasal spray 2-percent suspension for prevention and treatment of experimentally induced rhinovirus colds in healthy volunteers, *Antimicrob. Agents Chemother.* 47 (2003) 3907–3916, <https://doi.org/10.1128/AAC.47.12.3907-3916.2003>.
- [14] H. Yang, W. Xie, X. Xue, K. Yang, J. Ma, W. Liang, Q. Zhao, Z. Zhou, D. Pei, J. Zierbuhr, R. Hilgenfeld, K. Yung-Yuen, L. Wong, G. Gao, S. Chen, Z. Chen, D. Ma, M. Bartlam, Z. Rao, Design of wide-spectrum inhibitors targeting coronavirus main proteases, *PLoS Biol.* 3 (10) (2005) e324, <https://doi.org/10.1371/journal.pbio.0030324>.
- [15] C. Wu, Y. Liu, Y. Yang, P. Zhang, W. Zhong, Y. Wang, Q. Wang, Y. Xu, M. Li, M. Zheng, L. Chen, H. Li, Analysis of therapeutic targets for SARS-CoV-2 and discovery of potential drugs by computational methods, *Acta Pharm. Sin. B* (2020), <https://doi.org/10.1016/j.apsb.2020.02.008>.
- [16] M.T. Qamar, S.M. Alqahtani, M.A. Alamri, L.L. Chen, Structural basis of SARS-CoV-2 3CLpro and anti-COVID-19 drug discovery from medicinal plants, *Journal of Pharmaceutical Analysis* (2020), <https://doi.org/10.1016/j.jpha.2020.03.009>.
- [17] N. Chandak, P. Kumar, P. Kaushik, P. Varshney, C. Sharma, D. Kaushik, J. Sudha, K.R. Aneja, P.K. Sharma, Dual evaluation of some novel 2-amino-substituted coumarinylthiazoles as anti-inflammatory-antimicrobial agents and their docking studies with COX-1/COX-2 active sites, *Journal of Enzyme Inhibition and Medicinal Chemistry* 29 (2014) 476–484, <https://doi.org/10.3109/14756366.2013.805755>.
- [18] W.L. Jorgensen, The many roles of computation in drug discovery, *Science* 303 (2004) 1813–1818, <https://doi.org/10.1126/science.1096361>.
- [19] Schrödinger, QikProp 4.4 user manual, http://gohom.win/ManualHom/Schrodinger/Schrodinger_2015-2_docs/qikprop/qikprop_user_manual.pdf, (2015).
- [20] F. Ntie-Kang, C.V. Simoben, B. Karaman, V.F. Ngwa, P.N. Judson, W. Sippl, L.M.A. Mbaze, Pharmacophore modeling and in silico toxicity assessment of potential anticancer agents from African medicinal plants, *Drug Design, Development and Therapy* 10 (2016) 2137, <https://doi.org/10.2147/DDDT.S108118>.
- [21] J.E. Ridings, M.D. Barratt, R. Cary, C.G. Earnshaw, C.E. Eggington, M.K. Ellis, P.N. Judson, J.J. Langowski, C.A. Marchant, M.P. Payne, W.P. Watson, T.D. Yih, Computer prediction of possible toxic action from chemical structure: an update on the DEREK system, *Toxicology* 106 (1996) 267–279, [https://doi.org/10.1016/0300-483X\(95\)03190-Q](https://doi.org/10.1016/0300-483X(95)03190-Q).
- [22] N. Greene, P.N. Judson, J.J. Langowski, C.A. Marchant, Knowledge-based expert systems for toxicity and metabolism prediction: DEREK, STAR and METEOR, *SAR QSAR Environ. Res.* 10 (1999) 299–314, <https://doi.org/10.1080/10629369908039182>.
- [23] H. Eckert, J. Bajorath, Molecular similarity analysis in virtual screening: foundations, limitations and novel approaches, *Drug Discov. Today* 12 (2007) 225–233, <https://doi.org/10.1016/j.drudis.2007.01.011>.
- [24] J.W. Godden, L. Xue, J. Bajorath, Combinatorial preferences affect molecular similarity/diversity calculations using binary fingerprints and Tanimoto coefficients, *J. Chem. Inf. Comput. Sci.* 40 (2000) 163–166, <https://doi.org/10.1021/ci990316u>.
- [25] E.C. Padilha, R.B. Serafim, D.Y. Sarmiento, C.F. Santos, C.B. Santos, H.T.P. Carlos, New PPAR α / γ / δ optimal activator rationally designed by computational methods, *J. Braz. Chem. Soc.* 27 (2016) 1636–1647, <https://doi.org/10.5935/0103-5053.20160043>.
- [26] B.K. Shoichet, Virtual screening of chemical libraries problems with virtual screening, *Nature* 432 (7019) (2006) 862–865, <https://doi.org/10.1038/nature03197>.
- [27] J.V. Ferreira, G.A. Chaves, B.L. Marino, K.P. Sousa, L.R. Souza, M.F. Brito, H.R.C. Teixeira, C.H.T.P. da Silva, L.I. Hage-Melim, Cannabinoid type 1 receptor (CB1) ligands with therapeutic potential for withdrawal syndrome in chemical dependants of *Cannabis sativa*, *ChemMedChem* 12 (16) (2017) 1408–1416, <https://doi.org/10.1002/cmdc.201700129>.
- [28] J.M. Galúcio, E.F. Monteiro, D.A. de Jesus, C.H. Costa, R.C. Siqueira, G.B. dos Santos, J. Lameira, K.S. da Costa, In silico identification of natural products with anticancer activity using a chemo-structural database of Brazilian biodiversity, *Comput. Biol. Chem.* 83 (2019) 107102, <https://doi.org/10.1016/j.compbiolchem.2019.107102>.
- [29] H. Gao, S. Schneider, P. Andrews, K. Wang, X. Huang, B.A. Sparling, Virtual screening to identify potent septipierin reductase inhibitors, *Bioorg. Med. Chem. Lett.* 30 (2) (2020) 126793, <https://doi.org/10.1016/j.bmcl.2019.126793>.
- [30] E.V. Fagherazzi, A.V. Garcia, N. Maurmann, T. Bervanger, H.L. Halmenschlager, S.B. Busato, E.J. Hallak, W.A. Zuardi, A.J. Crippa, N. Schröder, Memory-rescuing effects of cannabidiol in an animal model of cognitive impairment relevant to neurodegenerative disorders, *Psychopharmacology* 219 (2012) 1133–1140, <https://doi.org/10.1007/s00213-011-2449-3>.
- [31] V. Hornak, C. Simmerling, Targeting structural flexibility in HIV-1 protease inhibitor binding, *Drug Discov. Today* 12 (2007) 132–138, <https://doi.org/10.1016/j.drudis.2006.12.011>.
- [32] M. Hoffmann, H. Kleine-Weber, S. Schroeder, N. Krüger, T. Herrler, S. Erichsen, T.S. Schiergens, G. Herrler, N.H. Wu, A. Nitsche, M.A. Müller, C. Drosten, S. Pohlmann, SARS-CoV-2 cell entry depends on ACE2 and TMPRSS2 and is blocked by a clinically proven protease inhibitor, *Cell* 181 (2020) 1–10, <https://doi.org/10.1016/j.cell.2020.02.052>.
- [33] B.E. Young, S.W.X. Ong, S. Kalimuddin, J.G. Low, S.Y. Tan, J. Loh, S.K. Lau, ... D.C. Lye, Epidemiologic features and clinical course of patients infected with SARS-CoV-2 in Singapore, *JAMA - Journal of the American Medical Association* (2020) 1–7, <https://doi.org/10.1001/jama.2020.3204>.
- [34] W. Muster, A. Breidenbach, H. Fischer, S. Kirchner, L. Müller, C. Pähler, Computational toxicology in drug development, *Drug Discov. Today* 13 (2008) 303–310, <https://doi.org/10.1016/j.drudis.2007.12.007>.
- [35] L. Zhang, D. Lin, X. Sun, U. Curth, C. Drosten, L. Sauerhering, S. Becker, K. Rox, R. Hilgenfeld, Crystal structure of SARS-CoV-2 main protease provides a basis for design of improved α -ketoamide inhibitors, *Science* (2020), <https://doi.org/10.1126/science.abb3405>.
- [36] Y. Furuta, T. Komeno, T. Nakamura, Favipiravir (T-705), a broad spectrum inhibitor of viral RNA polymerase, *Proceedings of the Japan Academy, Series B* 93 (2017) 449–463, <https://doi.org/10.2183/pjab.93.027>.
- [37] T. Nagata, A.K. Lefor, M. Hasegawa, M. Ishii, Favipiravir: a new medication for the Ebola virus disease pandemic, *Disaster Medicine and Public Health Preparedness* 9 (2015) 79–81, <https://doi.org/10.1017/dmp.2014.151>.
- [38] Y. Furuta, K. Takahashi, Y. Fukuda, M. Kuno, T. Kamiyama, K. Kozaki, N. Nomura, H. Egawa, S. Minami, Y. Watanabe, H. Narita, K. Shiraki, In vitro and in vivo activities of anti-influenza virus compound T-705, *Antimicrob. Agents Chemother.* 46 (2002) 977–981, <https://doi.org/10.1128/AAC.46.4.977-981.2002>.
- [39] E. Schrezenmeier, T. Dörner, Mechanisms of action of hydroxychloroquine and chloroquine: implications for rheumatology, *Nat. Rev. Rheumatol.* (2020) 1–12, <https://doi.org/10.1038/s41584-020-0372-x>.
- [40] A. Cortegiani, G. Ingoglia, M. Ippolito, A. Giarratano, S. Einav, A systematic review on the efficacy and safety of chloroquine for the treatment of COVID-19, *J. Crit. Care* (2020), <https://doi.org/10.1016/j.jccr.2020.03.005>.
- [41] J.C. Yam, A.K. Kwok, Ocular toxicity of hydroxychloroquine, *Hong Kong Med J* 12 (2006) 294–304, <https://doi.org/10.1080/08820530802049962>.
- [42] L. De Sistiernes, J. Hu, D.L. Rubin, M.F. Marmor, Localization of damage in progressive hydroxychloroquine retinopathy on and off the drug: inner versus outer retina, parafovea versus peripheral fovea, *Invest. Ophthalmol. Vis. Sci.* 56 (2015) 3415–3426, <https://doi.org/10.1167/iov.14-16345>.
- [43] M.H. Weeks, T.O. Downing, N.P. Musselman, T.R. Carson, W.A. Groff, The effects of continuous exposure of animals to ethanolamine vapor, *Am. Ind. Hyg. Assoc. J.* 21 (1960) 374–381, <https://doi.org/10.1080/00208896009344089>.
- [44] P. Sang, S.H. Tian, Z.H. Meng, L.Q. Yang, Insight derived from molecular docking and molecular dynamics simulations into the binding interactions between HIV-1 protease inhibitor s and SARS-CoV-2 3CLpro, *ChemRxiv* (2020), <https://doi.org/10.26434/chemrxiv.11932995.v1>.
- [45] S.P. Singh, B.K. Konwar, Molecular docking, DFT and ADME-toxicity studies on analogues of epigallocatechin gallate as SARS coronavirus 3CL protease inhibitors, *Journal of Bioinformatics and Intelligent Control* 2 (2013) 1–10, <https://doi.org/10.1166/jbic.2013.1030>.
- [46] A. Fischer, M. Sellner, S. Naranjan, M.A. Lill, M. Smieško, Inhibitors for Novel Coronavirus Protease Identified by Virtual Screening of 687 Million Compounds, *chemrxiv.org*.
- [47] S. Jo, S. Kim, D.H. Shin, M.S. Kim, Inhibition of SARS-CoV 3CL protease by flavonoids, *Journal of Enzyme Inhibition and Medicinal Chemistry* 35 (2020) 145–151, <https://doi.org/10.1080/14756366.2019.1690480>.
- [48] P. Gautret, J.C. Lagier, P. Parola, L. Meddeb, M. Mailhe, B. Doudier, J. Courjon, V. Giordanengo, E.V. Vieira, H.T. Dupont, S. Honoré, P. Colson, E. Chabriere, B. La Scola, J.M. Rolain, P. Brouqui, D. Raouf, Hydroxychloroquine and azithromycin as a treatment of COVID-19: results of an open-label non-randomized clinical trial, *Int. J. Antimicrob. Agents* (2020) 105949, <https://doi.org/10.1016/j.ijantimicag.2020.105949>.
- [49] A.T. Ton, F. Gentile, M. Hsing, F. Ban, A. Cherkasov, Rapid identification of potential inhibitors of SARS-CoV-2 main protease by deep docking of 1.3 billion compounds, *Mol Inform* (2020), <https://doi.org/10.1002/minf.202000028>.
- [50] K.H. Bleicher, H.J. Böhm, K. Müller, A.I. Alanine, Hit and lead generation: beyond high-throughput screening, *Nat. Rev. Drug Discov.* 2 (2003) 369–378, <https://doi.org/10.1038/nrd1086>.

- [51] Z.A. Fazeel, Apixaban: an oral anticoagulant having unique mechanism of action with better safety and efficacy profile, *MAMC Journal of Medical Sciences* 2 (2016) 63, <https://doi.org/10.4103/2394-7438.182723>.
- [52] N. Tang, H. Bai, X. Chen, J. Gong, D. Li, Z. Sun, Anticoagulant treatment is associated with decreased mortality in severe coronavirus disease 2019 patients with coagulopathy, *J. Thromb. Haemost.* (2020), <https://doi.org/10.1111/jth.14817>.
- [53] S.H. Hohnloser, M. Fudim, J.H. Alexander, D.M. Wojdyla, J.A. Ezekowitz, M. Hanna, D. Atar, Z. Hijazi, M.C. Bahit, S.M. Al-Khatib, J.L. Lopez-Sendon, L. Wallentin, C.B. Granger, R.D. Lopes, Efficacy and safety of Apixaban versus warfarin in patients with atrial fibrillation and extremes in body weight, *Circulation* 139 (2019) 2292–2300, <https://doi.org/10.1161/CIRCULATIONAHA.118.037955>.